PCCP

Accepted Manuscript

ROYAL SOCIETY OF CHEMISTRY

www.rsc.org/pccp

Journal Name

RSCPublishing

ARTICLE

Insight into Structure and Stability of DNA in Ionic Liquids from Molecular Dynamics Simulation and Experimental Studies

Cite this: DOI: 10.1039/xoxxoooooox

Received ooth January 2012,
Accepted ooth January 2012

DOI: 10.1039/xoxxoooooox

www.rsc.org/

K. Jumbri,[a,b] M. B. Abdul Rahman,[a,b] E. Abdulmalek,[a,b] H. Ahmad[a,b] and N. M. Micaelo[c,*]

Molecular dynamics simulation and biophysical analysis were employed to reveal the characteristics and influence of ionic liquids (ILs) on the structural properties of DNA. Both computational and experimental evidences indicate that DNA retains its native B-conformation in ILs. Simulation data shows that the hydration shells around the DNA phosphate group were the main criterion for DNA stabilization in this ionic media. Stronger hydration shells reduce the binding ability of ILs' cations to the DNA phosphate group, thus destabilizing the DNA. The simulation results also indicated that DNA structure maintain its duplex conformation when solvated by ILs at different temperatures up to 373.15 K. The result further suggests that the thermal stability of DNA at high temperatures is related to the solvent thermodynamics, especially entropy and enthalpy of water. All the molecular simulation results were consistent with the experimental findings. Understanding of IL-DNA properties could be used as a platform for future development of specific ILs for nucleic acids technology.

1. Introduction

DNA is generally more stable than RNA in common conditions. The hydroxyl groups in RNA make RNA less stable because it is more prone to hydrolysis. However, there are many factors that affect the stability and conformation of nucleic acids especially DNA. Slow hydrolytic reactions such as deamination and depurination can damage the double-helix of DNA.[1] Physical factors such as ionic strength, pH, temperature and solvent can disturb the helical structure and cause denaturation.[2,3] Additionally, traditional extractions with chloroform/phenol[4] can also cause denaturation of DNA during the extraction process. More importantly, the contamination of extracted DNA by organic solvents is unavoidable and creates vital problems for the biological investigations as traditional organic solvents are known to be toxic to bioprocesses.[5,6]

Although DNA is considered stable in an aqueous solution, a few studies have reported on the stability of DNA in a various of non-aqueous and mixed solvents, revealing that DNA is not stable and loses its native B-helical structure when dissolved in formamide, methanol or dimethyl sulfoxide.[7,8] Duplex DNA in aqueous solution was found to be unstable when stored for several months[9] and the stability of DNA is also affected by temperature.[10] The dry storage of nucleic acids, which utilizes the basic concept of anhydrobiosis is an alternative to the old-style cold-storage DNA.[11] Therefore, the development of new non-aqueous media that can stabilize and maintain DNA for a long period especially at room temperature, is increasing.

During the last decade, ILs have proven to be the preferred solvents to replace traditional organic solvents and aqueous solution in many types of reactions. ILs contain a mixture of cations and anions, and can be ecologically green solvents due to their physico-chemical properties such as low vapour pressure, non-flammability, high chemical and thermal stability, low toxicity, high ionic conductivity, controllable hydrophobicity and hydrophilicity.[12,13] Based on their properties, ILs had been used in reactions such organic synthesis,[14-17] electrochemistry,[18,19] extraction/separation,[20-23] material preparation[24-28] and many more. In the past few years, a number of publications reported the use of ILs in life sciences involving the separation and extraction of nucleic acids, especially DNA.[29-33]

DNA in ILs was reported for the first time by Qin and Li.[29] An ionic liquid-coated capillary was designed specifically for DNA separation based on electrostatic interactions between DNA strands and alkylimidazolium-based ILs. Similar studies also reported the use of ILs in designing ion conductive DNA films.[30] Both earlier studies indicate that DNA can be separated by ILs, using electrochemistry method. Later studies explored the extraction of trace amounts of double-stranded DNA by using ILs from an aqueous solution.[31] Interaction between the P-O bonds of phosphate groups in the DNA strands was

confirmed through ^{31}P NMR and fourier transform-infrared spectroscopy (FT-IR). The authors[31] also identified that protein and metal species do not interfere with the extraction process. This finding provides an alternate approach for the measurement of DNA in ILs as well as separation/purification of trace amounts of DNA in real-world biological matrixes. Meanwhile, MacFarlene et al.[9] used spectroscopy to study the stability of DNA in hydrated ILs. They demonstrated that the structural and chemical stability of DNA are preserved for up to a year in a series of hydrated choline-based ILs. The binding characteristics and molecular mechanism of the interaction between a typical IL, 1-butyl-3-methylimidazolium chloride ([bmim][Cl]) and DNA were systematically investigated by Ding et al.[33] Although their work provides useful information about the interaction between ILs and DNA, the molecular mechanism of the interaction was still not clear. Furthermore, the computational approach does not detail the solvation interaction, stability and flexibility of DNA.

Until now, the properties of DNA in ILs from theoretical point of view have not been well studied. Thus far, only two research groups have successfully performed the MD simulation of DNA in ILs. Our previous work shows the important role of cations, anions and the hydrogen-bonding interactions of the cations with the DNA bases in the stability of Drew Dickerson B-DNA in neat of various ILs[34]. Later, Chandran et al.[35] employed MD simulations with the support of spectroscopic experiments to unravel the key factors that stabilize DNA in different hydrated ionic liquid [C_4mim]Cl. In comparison, there was slightly different in term of stability of calf thymus DNA in [C_4mim]Cl and in our [$C_n$bim]Br ILs. Increasing alkyl chain length of cation helps to increase the stability of DNA. As reported, RMSD value of Calf thymus DNA in 80 % (w/w) [C_4mim]Cl is slightly higher (0.153 nm)[35] than in 75 % [C_4bim]Br (RMSD of 0.143 nm) from our present work. This reveals that alkyl chain length of ILs cation also play a small role in DNA stability. Although their work revealed about the mechanism of DNA solvation and stabilization by ILs, the effect of temperature on the stability of duplex DNA in ILs are still unknown. Therefore, in this study the combination of both MD simulations and spectroscopy were employed to expose the behaviour of DNA in ILs with particular focus on the effect of water content and temperature on the stability and dynamics of DNA.

2. Theoretical and Experimental Section

2.1 Simulation Details

The structure of Calf-thymus DNA (Ct-DNA) was obtained from a RCSB Protein Data Bank (RCSB PDB) with a PDB ID 425D.[36] The Ct-DNA was chosen due to recent experimental evidence about the behaviour of this DNA in ILs.[33,37] To build the initial structure, a cubic box was used and the size of the box was calculated based on a cut-off of 1.2 nm. The DNA was placed at the center of a 6.7 x 6.7 x 6.7 nm box and solvated in three different neat ILs [C_2bim]Br, [C_4bim]Br and [C_6bim]Br. In the control simulation, DNA was simulated in an aqueous system using the TIP4P model of water.

Since water activity plays an important role in the stabilization of DNA, the effect of water in hydrated ILs was also studied. Only one IL [C_4bim]Br was selected as a model for this purpose. Subsequently, three additional simulations were performed by varying the ratio of IL:water. The number of molecules required in a given simulation box were calculated based on percentage weight of IL over weight of water (% w/w). For the DNA in IL:water systems, the equilibrated DNA structure with a layer of surrounding water molecules within 0.35 nm from DNA surface taken from the trajectory of a MD simulation in water was placed into a simulation box. The box was then filled with the requisite number of IL pair and water molecules to reach the desired IL concentrations. Further details of the systems are listed in Table 1. In the aqueous system, the concentration of solution was set to 100 mM by replacing a selected water molecule by sodium and chloride ions. The OPLS force field and TIP4P water model were adopted to represent the interaction potentials of DNA and water, respectively. The ILs were modeled using a similar parameterization approach to that previously used.[38] Details of the ILs parameterization and validation are described in the Supporting Information.

Table 1. Number of molecules used in the simulation.

System	[IL]:H2O (% w/w)	Number of molecules		
		Cation	Anion	TIP4P
[C_2bim]Br	100:0	962	940	-
[C_4bim]Br	100:0	826	804	-
[C_6bim]Br	100:0	737	715	-
H_2O	0:100	40 Na	18 Cl	9637
[C_4bim]Br	25:75	223	201	7108
[C_4bim]Br	50:50	424	402	4840
[C_4bim]Br	75:25	625	603	2420

22 sodium atoms were used as counter ion to neutralize the DNA charges. The remaining 18 sodium and 18 chlorine atoms were used to set 100 mM concentration of aqueous system.

The parameters used in MD simulation are as follows. The integration step of 2 fs was used. Non-bonded interactions were calculated up to 1.2 nm and long-range electrostatic interactions were treated with Particle-Mesh Ewald (PME)[39,40] with a grid spacing of 0.12 nm and fourth-order interpolation. Neighbor searching was done up to 1.2 nm and updated every five steps. Bond lengths were constrained with LINCS.[41] Temperature and pressure control were implemented using the Berendsen thermostat and Berendsen barostat, respectively.[42] The reference pressure of 1 atm and relaxation time of 2.0 ps were applied. Isothermal compressibility for pressure control was set at 4.5×10^{-5} bar^{-1}. The heat was separated in two heat baths with temperature coupling constants of 0.1 ps.

A few steps of energy minimization were performed. Each system was energy minimized with 5000 steps of the steepest descent followed by 5000 steps of conjugate gradient. All heavy atoms of DNA were position restrained with a force constant of 10^6 kJ/mol^{-1} nm^{-2}. The system was further minimized with 5000 steps of steepest descent with position

restraints applied to the DNA main chain atoms with the same force constant as previously mentioned. The main chain atom selection includes all phosphorous and oxygen atoms of the phosphate groups and the connecting atoms of the sugar residues. The system was then energy minimized without applying any position restraints with 5000 steps of steepest descent followed by 5000 conjugate gradients.

The simulation of DNA in different systems was initialized in the canonical ensemble (NVT) for 500 ps. The position restraints were applied to all heavy atoms with a force constant of 10^6 kJ/mol^{-1} nm^{-2}. The isobaric-isothermal (NPT) was then introduced to the system during 100 ps simulation time while the DNA main chains was restrained with the same force constant. For production simulation, the NPT ensemble was introduced. The simulations were performed for 10 ns at various temperatures, 298.15, 323.15, 343.15 and 373.15 K. The system reached equilibrium in the first 6-8 ns due to the slow dynamics that characterize this type of solvent. The trajectory for all analyses was taken from the last 2 ns. All MD simulations here were performed with the GROMACS package version 4.5.

The root mean square deviation (RMSD) of DNA was calculated by fitting the simulated duplex DNA against the initial X-ray crystal structure. Radial distribution function (RDF) was determined between the residues' centre-of-mass (RES-COM) of cation/anion around the DNA phosphate region. Hydrogen bonding interaction was determined between the DNA bases and the polar proton in imidazole ring. The alkyl chains of cations were not considered to have any hydrogen bond interactions with the DNA bases. The bromide anion was considered a hydrogen-bond-acceptor since it has available electron pairs. The hydrogen bond interaction between the anion and DNA base was also calculated. A hydrogen bond is considered to exist in one conformation if the distance between the hydrogen atom and the acceptor is less than 0.35 nm and the angle formed by acceptor-donor-hydrogen is less than 30°. Hydrogen bond interactions were calculated as an average. All pictures shown were created by Pymol.[43]

2.2 Experimental Details

2.2.1 Materials

1-butylimidazole, 1-bromobutane and the fluorescence probe pyrene were purchased from Sigma-Aldrich with high purity (99 %). 1,3-dibutylimidazolium bromide ([C_4bim]Br) IL was synthesized and purified according to method published by Wang et al.[44] Calf-thymus DNA (Ct-DNA, ~10 kbp, D1501) was purchased from Sigma and used without further treatment since the purity was high as determined by UV-visible. The ratio of the absorbance of the DNA stock solution at wavelengths 260 nm and 280 nm was found to be 1.9, indicating the absence of protein contamination. Other chemicals employed in this work were of analytical grade and were used without further purification. Deionized water type III was used (Super Q Millipore system, conductivity lower than 18 μs cm^{-1}).

The solution for fluorescence analysis contained 8 % (w/w) ethanol for pyrene solubility. Ethanol can stabilize DNA and prevent its denaturation, which could be favoured in the absence of a buffer or supporting electrolyte.[45] Stock solution of DNA was prepared by dissolving Ct-DNA in deionized water and stored at 4° C with gentle shaking for 24 hours to achieve homogeneity. DNA concentration was determined by using the extinction coefficient of 6600 M^{-1} cm^{-1} at 260 nm and expressed in terms of base molarity.[46] The DNA stock solution was stored in a freezer at -20 °C and used within a month.

2.2.2 Fluorescence Emission

The fluorescence emission spectra of DNA-bound pyrene and free pyrene were recorded by a Cary Eclipse Fluorescence Spectrophotometer. The concentration of pyrene in aqueous solution containing 8 % ethanol was kept constant at 0.5 μM. Both the excitation and emission were set at wavelengths 335 and 373 nm, respectively. Band slits were fixed at 5.0 nm and the fluorescence spectra were corrected for the background intensities of the solution without DNA. A 1.0 cm light-path quartz cuvette was used. The DNA-bound pyrene was prepared by titrating an aqueous solution of Ct-DNA into the solution of pyrene. Emission intensity of pyrene decreased upon the addition of Ct-DNA and remained constant during saturation, indicating that all the pyrene was bound to DNA. Then, 0.5 M solution of [C_4bim]Br was slowly titrated into the solution of DNA-bound pyrene and the emission intensity of free pyrene was observed.

2.2.3 Circular Dichroism

Circular dichroism (CD) spectra of Ct-DNA in different percentages of [C_4bim]Br in water (25, 50 and 75 % w/w) were recorded using Jasco J-815 Circular Dichroism spectrometer equipped with Peltier Temperature Controller (PTC-423s) and a water circulation unit. A rectangular quartz cell of 1.0 cm path length was used. Titrations of [C_4bim]Br into DNA in aqueous solution were performed with a fixed concentration of Ct-DNA (0.3 mM). Spectra shown are averaged over three scans with scan speed was set at 50 nm/min and wavelengths from 320 to 240 nm. Band width was set at 1.0 nm and standard sensitivity was used. An appropriate blank was subtracted from respective spectra and the data was subject to noise reduction analysis.

3. Results and Discussion

3.1 Finding from MD Simulation

3.1.1 Structural Modelling of DNA in ILs

The structural stability of B-conformation Ct-DNA was investigated by comparing the atomic RMSD of DNA (all heavy atoms) solvated in neat ILs relative to the initial position in the crystal structure, as shown in Figure 1. On average over the last 2 ns, all RMSD values calculated for DNA in each ILs were found to be lower than those observed in an aqueous system (averaged $RMSD_{in\ neat\ ILs}$ = 0.143 nm and $RMSD_{in\ water}$ = 0.290 nm). Increasing carbon chain cations from C_2 to C_6 seems to slightly decrease the RMSD of DNA.This indicates that alkyl

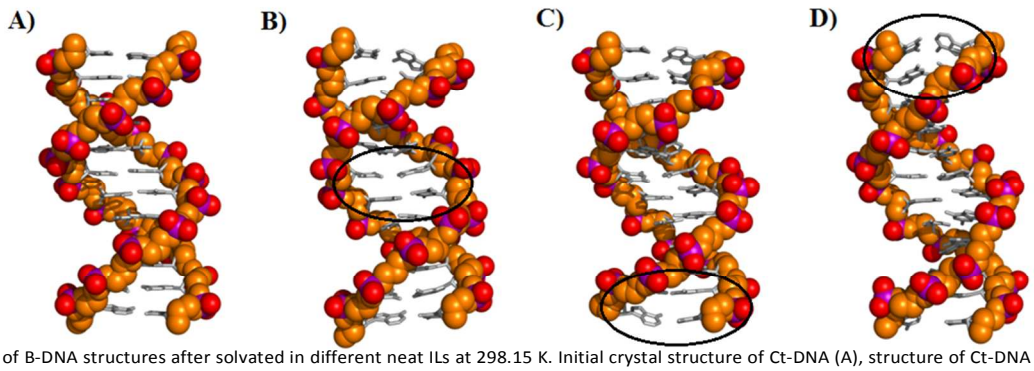

Fig. 2 Comparison of B-DNA structures after solvated in different neat ILs at 298.15 K. Initial crystal structure of Ct-DNA (A), structure of Ct-DNA in neat [C_2bim]Br (B), [C_4bim]Br (C) and [C_6bim]Br (D). The circles show that the bases in DNA strands located at head and tail were most disturbed by ILs molecules in comparison to the bases in the middle of DNA strands. The backbone of DNA consists of phosphate groups able to maintain its helical shape due to the strong electrostatic attraction formed between ILs' cation and DNA phosphate groups (See section 3.1.3 for details about electrostatic attraction). Colour schemes are as follow: red, oxygen; magenta, phosphorus; orange, backbone of DNA and gray, DNA bases. The structure of DNA in each ILs was taken from the final conformations of a 10 ns MD simulation trajectory.

chains lengths of cations have a small influence on the stability of B-DNA. For an inspection, the structure of duplex DNA solvated in different neat ILs was also taken from final conformations of a 10 ns MD simulation trajectories and its conformation was compared with the crystal structure as shown in Figure 2. The figure shows that the structures were stable and the sampled configurations were similar to the initial structure. Both finding demonstrate that DNA maintains its B-native structure in neat ILs and corroborates with our previous simulation finding, where we have noted the existence of native DNA conformation in a variety of neat ILs at 298.15 K.[34]

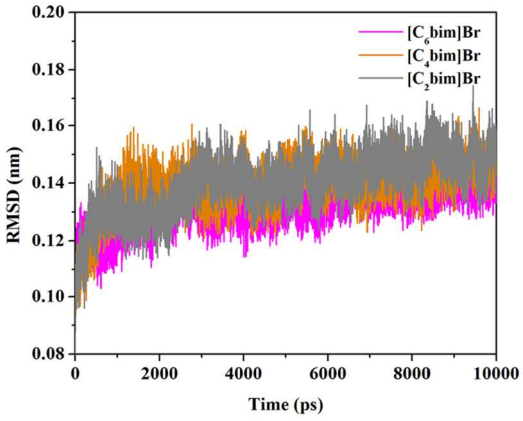

Fig 1. RMSD (nm) of duplex Ct-DNA (all heavy atoms) solvated by three neat ILs at 298.15 K.

Since ILs are well known to be thermally stable, the simulation of DNA in neat IL [C_4bim]Br was also performed at different temperatures. Interestingly, it was observed that the average RMSD of DNA slightly increases with increasing temperature as shown in Figure 3, indicating that ILs is able to stabilize DNA and maintain its native B-conformation at temperature up to 373.15 K. MD simulation of DNA in hydrated ILs was also performed. For this purpose, only [C_4bim]Br was selected as a model in order to further study the structural stability and dynamics of double helical DNA structure in a mixture of IL and water. The average RMSD of DNA (all heavy atoms) solvated in different percentages of [C_4bim]Br (25, 50 and 75 % w/w) at various temperatures is depicted in Figure 4.

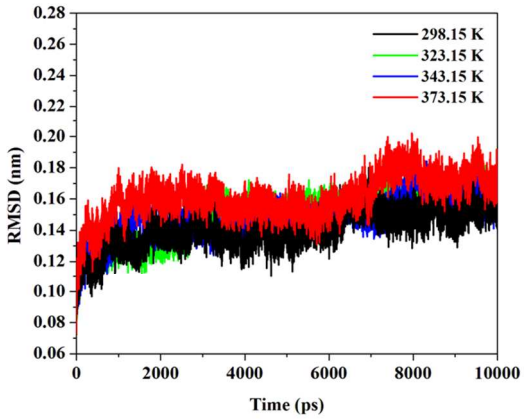

Fig. 3 RMSD (nm) of duplex Ct-DNA (all heavy atoms) simulated in neat [C_4bim]Br at various temperatures.

At 298.15 K, the average RMSD of DNA in 75 % (w/w) [C_4bim]Br solution was found to be only 0.169 nm. Even in adilute solution of 25 % and 50 %, average RMSD of DNA was lower, 0.232 and 0.222 nm respectively. The results imply that increasing percentages of [C_4bim]Br result in more native-like DNA structure. It shows that DNA in all percentages of [C_4bim]Br solution have RMSD smaller than the average RMSD of DNA in an aqueous system (0.290 nm), suggesting that DNA retains its native conformation at 298.15 K, which is in good agreement with spectroscopic findings (see Experimental Verifications in this paper).

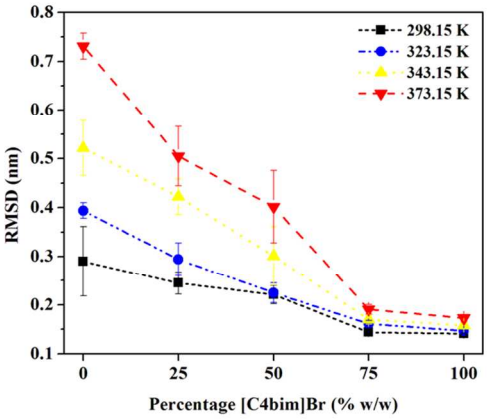

Fig. 4 Average RMSD (nm) of Ct-DNA (all heavy atoms) solvated in different percentages of hydrated [C_4bim]Br solution (25, 50 and 75 % w/w) at various temperatures. For comparison, simulation of Ct-DNA in aqueous system is shown at zero percentage of [C_4bim]Br. Values are averages over the last 2 ns of MD simulation.

Although the average RMSD of DNA increases with increasing temperature, DNA in 75 % IL solution shows RMSD of DNA at 373.15 K is even lower than the RMSD of DNA in an aqueous system at 298.15 K. Interestingly, this result indicated that DNA maintains its native conformation even at high temperatures in the presence of a small amount of water, as was observed in proteins.[47-49] The data corroborated well with the experimental evidence from MacFarlene et al.[9] who reported that DNA is stable and retains its B-conformation in hydrated choline-based ILs. Meanwhile, DNA in 50 % (w/w) [C_4bim]Br solution at 323.15 K shows that RMSD of DNA was lower than RMSD of DNA in water at 298.15 K.

As observed, it is clear that the stability of Ct-DNA is mainly dependant on the water content, or more specifically the properties of hydration shells around DNA. To understand this hypothesis, the distribution of cations on Ct-DNA surface, picked up at 10 ns was investigated as illustrated in Figure 5. It is evident that, populations of cations were not only located near the DNA phosphate groups due to the charge attraction, but also associate with the major groove of DNA. Interestingly, a few $[C_4bim]^+$ ions were also observed in the minor groove as well. This implies that the surrounding cations around DNA surface entered the major and minor grooves by disrupting the hydration shells and remained bound to the grooves without disturbing the helical structure of DNA. Not surprisingly, the population of $[C_4bim]^+$ was found to be slightly higher in the wider major groove than the narrower minor groove.

It was observed that the hydrocarbon chains of cation were perpendicular to the surface of DNA and formed hydrophobic interactions with the DNA bases. This observation was supported by the experimental evidence of Ding et al.[33] and Wang et al.[37] who pointed out that hydrophobic interactions formed between hydrocarbon chains of the ILs and DNA bases. Since cations were also detected in both grooves, the hydrogen bonding together with contribution of hydrophobic interactions between cation-grooves might also assist in stabilizing the DNA.

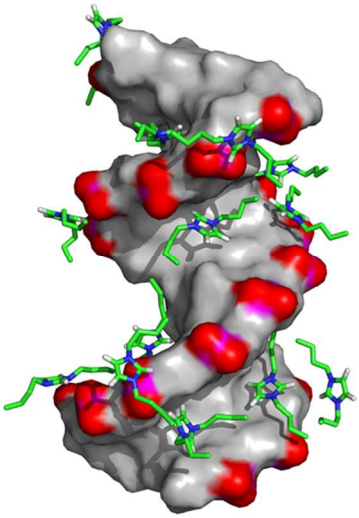

Fig. 5 Representative distribution of $[C_4bim]^+$ molecules showing their association with the B-DNA phosphate groups, major and minor grooves. The distribution of anions (Br^-) molecules was not shown here. Colour schemes are as follow: red, oxygen; magenta, phosphorus; gray, DNA structure; green, carbon; blue; nitrogen and white; proton. Figure made from the final conformations of a 10 ns MD simulation trajectory.

3.1.2 Role of Hydration Shells

Based on the current work, it is obvious that hydration shells play a vital role in stabilizing or destabilizing DNA and their conformational dynamics. Figure 6 shows representative distribution of cation and water molecules in the solvation layers of DNA, defined as a shell of 0.35 nm. The figure clearly illustrated that at 25 % and 50 % [C_4bim]Br solution, accumulation of water surrounding the DNA surface is high as compared to cations, thus the arrangement of water molecules form strong hydration shell (Figure 6A and 6B). In 75 % IL solution, $[C_4bim]^+$ cations were able to penetrate the hydration layer and take part in solvation mechanism (Figure 6C).

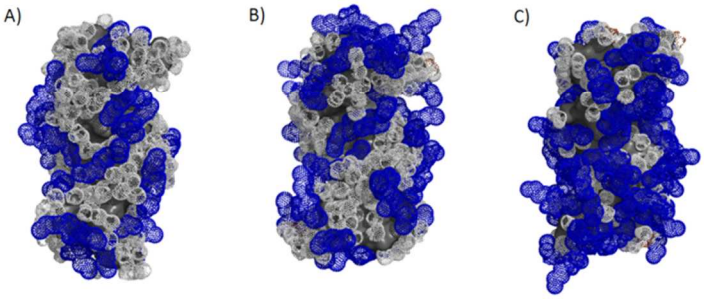

Fig. 6 Representative populations of cations and water molecules within 0.35 nm of DNA surface. A) 25 %, B) 50 % and C) 75 % (w/w) [C_4bim]Br solutions at 298.15 K. Colour scheme are as follow: white, water; blue, cation. Figures were taken from the final conformations of a 10 ns MD simulation trajectory.

At low relative humidity, water does not diffuse freely and mostly located around DNA phosphate groups.[50,51] In the presence of bulk [C_4bim]Br molecules, many hydrophobic tail of $[C_4bim]^+$ cation get stuck in the hydrophobic sugar-rich region via hydrophobic interaction. This interaction thereby

blocks the water passageway across to the amine bases. Water has more difficulty diffusing inside the helical structure and therefore disturbs the amine stacking less.[52] Thus, the disturbing of DNA conformation by water diffusion is reduced. Such a partial dehydration of DNA by [C_4bim]Br also could prevent hydrolytic reactions such as depurination and deamination. However, with increasing the water percentages, many water molecules can cross the hydrophobic sugar-rich region and formed "spine of hydration", especially in the DNA minor groove.[53,54] This will cause the diffusion of water molecules inside the helical structure increases and disturbs the amine stacking more. As a result, the double helical B-DNA structure change with increasing percentage of water (shown in Figure SS1 in Supporting Information), but retains its native B-conformation.

To further understand the role of hydration shells in DNA stability, the distribution of [C_4bim]Br and water molecules around DNA surface was calculated (see Table SS1 in Supporting Information file). In 25, 50 and 75 % [C_4bim]Br solutions, on average, 6.6, 9.4 and 13.9 molecules of cations were observed entering the hydration layers and getting involved in DNA solvation, respectively. Anions were virtually absent in the hydration layers with the average being 0.5 in 25 % [C_4bim]Br solution at any temperature. As the temperature is increased from 298.15 to 373.15 K, it was found that 16 and 30 water molecules were removed from the hydration layers by 25 and 50 % IL solutions.

However, the average numbers of [C_4bim]Br ions in the hydration layers remained unchanged with increasing temperature in 25 % and in 50 %, suggesting three possible explanations. First, this implies that incrementing the simulation temperature does not seem to affect the localization of cations round DNA surface. Second, any interactions between cations and DNA are not broken and are maintained in the hydration layers. Third, the remaining water molecules still formed strong hydration shells, thus preventing other cations to enter and disrupting the well-coordinated hydration layers.

With the increase in IL concentration, the population of [C_4bim]Br rises significantly. At high concentration (75 % w/w), the average number of [C_4bim]Br molecules in the solvation layers increases significantly with increasing temperature while the average number of water molecules greatly reduce from 128.5 to 94.5. At 75 % IL solution, the hydration shells become weaker. The arrangement of water molecules or the so-called "cone of hydration," the tetrahedral arrangement in the hydration layers especially on the surface of DNA phosphate groups,[55] was greatly disturbed by the penetration of ILs' cations. Many $[C_4bim]^+$ cations can compete for binding to the DNA phosphate groups, forming strong electrostatic interactions. The competition might also take place in the DNA major and minor grooves, which are rich with hydrogen donors/acceptors. Figure 7 shows the penetration of cation molecules into DNA minor groove in different percentages of [C_4bim]Br solution.

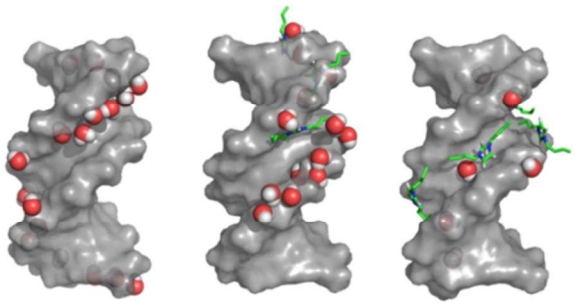

Fig. 7 Spin of hydration layers of water in the minor groove of Ct-DNA from control simulation (left). Penetration of hydration layers by $[C_4bim]^+$ cations at the minor groove in 25 % (mid) and 75 % (right) of [C_4bim]Br solutions.

It can be said that electrostatic interactions in combination with hydrogen bonding helps to stabilize duplex DNA. This finding is in agreement with Korolev et al.[56] that the hydration shells was the main factor for ionic binding to the phosphate groups of DNA, as well with X-ray studies.[57] Overall, it shows that from the data in Table SS1, the higher accumulation of cations over anions was observed due to less available space filled by cation molecules and neighbouring cation layers.

The percentage of water molecules stripped from the DNA hydration layers was calculated as a function of time and temperature. As depicted in Figure 8, at 298.15 K, cations stripped about 60 % of water molecules from the surface of DNA in 75 % [C_4bim]Br solution, averaged over the last 2 ns of the simulations. The percentage of water stripped increased up to 70 % when the temperature was increased to 323.15 K. This indicates that increasing the temperature leads increased penetration of [C_4bim]Br molecules into the hydration shells, which replaced the water molecules. However, the percentage of water stripped remained constant at 343.15 and 373.15 K, possibly due to the remaining water molecules that are retained in the deep hydration layers. At 25 and 50 % IL solutions, about 30 % and 45 % of the water molecules were stripped from the hydration shells at any temperature, demonstrating that at low and medium percentages of IL solutions, the hydration shells are strong even at high temperatures.

It is well known that the double-helical DNA structure melts into an open coil at high temperatures. Prior MD simulations have revealed that the thermal stability of DNA is mainly due to the hydration shells on DNA surface. Specifically, it is related to the solvent thermodynamics, especially entropy and enthalpy of water. As reported by Auffinger et al.[58] increasing the entropy of water will overcome enthalpy stabilization, leading to a pre-melting of the solvent that facilitates duplex disruption. Generally, entropy of water rapidly increases with increasing temperature. When the water content is high (in solution of 25 % [C_4bim]Br solution), the entropy of water molecules surrounding the duplex DNA especially the DNA phosphate groups increases with temperature, by reducing the number and strength of the solvent-solute (H_2O-DNA) interactions.

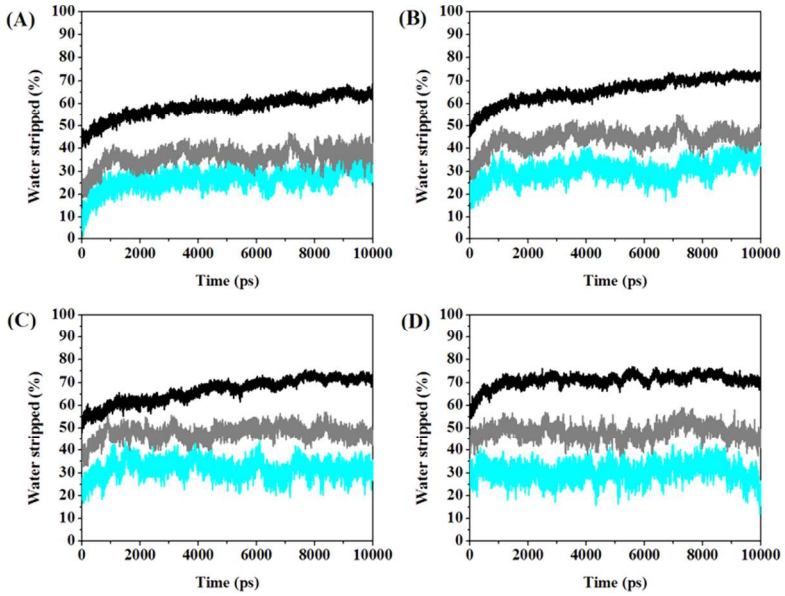

Fig. 8 Percentage of water stripped from the DNA surface at different percentages of [C4bim]Br in solution and at different temperatures. A) 298.15 K, B) 323.15 K, C) 343.15 K and D) 373.15 K. Colour scheme: black, 75 %; gray, 50 % and cyan, 25 % [C4bim]Br solution. The percentage of water molecules stripped from DNA surface was calculated from the fraction of water present within 0.35 nm located from DNA surface divided with the initial water count in the same distance. Data for analysis was taken from the last 2 ns simulation trajectories.

With further temperature increases, water molecules lose their cohesion where the solvent-solute is no longer sufficiently strong to stabilize the interactions, thus destabilizing the DNA structure. Referring back to Figure 4, the RMSD of DNA in hydrated 25 % [C_4bim]Br solution increases dramatically with temperature, indicating that the duplex DNA was not stable and the weakest structural elements of DNA system start to melt or undergo a helix-to-coil transition upon heating. Conversely, at low water content in 75 % [C_4bim]Br solution, the DNA phosphate group was surrounded and occupied by [C_4bim]$^+$ cations rather than water. Therefore, the increasing entropy of water does not affect the interaction between solvent-solute (in this case, the population of cations around the DNA surface were higher than water, therefore the major interaction is between [C_4bim]$^+$ cations and DNA) as the ILs have high thermal stability. The cation-DNA interaction was said stable and maintained even at higher temperature. Based on the MD data, it was found that 75 % IL solution was a suitable media for stabilizing the duplex DNA structure. This finding is in agreement with experimental work carried out by MacFarlene et al.[9]

3.1.3 Binding Characteristics of ILs-DNA

To understand the binding pattern of ILs to DNA, we considered the RDF of cation and anion around DNA surface. Centre of mass RDF (COM-RDFs) shows that alkylimidazolium cations in neat ILs interact most frequently with the DNA phosphate backbone groups. The radial

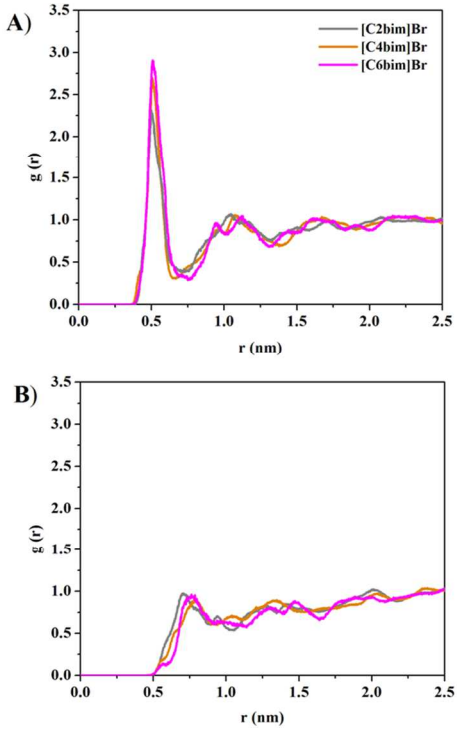

Fig. 9 (A) ILs' cations (head charge group) COM-RDF around DNA phosphate groups. (B) Exclusion of ILs' anions COM-RDF in the same region. Colour scheme: gray, [C_2bim]Br; orange, [C_4bim]Br and magenta, [C_6bim]Br.

distributions of the cations show a preferential localization of the cation "head" group located at 0.5 nm from the DNA phosphate groups (Figure 9A) and a complete exclusion of anion's molecules from this region (Figure 9B). The average coordination number indicated that there was no significant different in the cumulative number of each cations around DNA phosphate groups. On average, only one cation was observed in each simulation systems within a distance of 0.5 nm from negative charges of DNA phosphate groups.

The calculated interaction energies between different parts in the simulation systems (Table SS2, Supporting Information) show that the electrostatic attraction between IL's cation and DNA phosphate groups is more negative compared to interaction between water and DNA. This confirmed that the electrostatic attraction formed between IL and DNA has a major contribution to the DNA stability. This discovery is in agreement with our previous research on DNA in ILs[34] and correlates well with the ^{31}P NMR and FT-IR spectra studies confirming the major electrostatic interactions between the cation head group of $[bmim]^+$ with the phosphate groups of DNA.[31,33] Further research by Wang et al.[37] reveals that the major contribution to the binding Gibbs energy of the ILs to DNA also corresponds to the strong electrostatic interaction between the cationic head group of the ILs' cations and DNA.

3.1.2 Flexibility of B-DNA in ILs

Root mean square fluctuations (RMSF) of DNA bases in a series of hydrated [C_4bim]Br solutions were also calculated. RMSF also can locate the regions with high or low mobility based on the fluctuation of the position each DNA base relative to the average structure. RMSF of each DNA bases in neat and hydrated [C_4bim]Br solutions are shown in Figure SS2 in Supporting Information file. Duplex DNA was observed to have lower flexibility in hydrated [C_4bim]Br at low water percentage and neat [C_4bim]Br. Fluctuation of DNA bases decreases with increasing percentage of [C_4bim]Br solution. At 25 % (w/w), higher fluctuations occur, for the most part, in the heads and tails of DNA strands. Increasing the temperatures from 298.15 K to 373.15 K results in significant increments in fluctuations (Figure SS1A).

At 50 %, high fluctuations were still observed (Figure SS2B in Supporting Information file). However, the fluctuations of DNA bases in the heads and tails of DNA strands at 343.15 K and 373.15 K were found to be slightly lower than in 25 % [C_4bim]Br, indicating that the opening of base pairs might occur at high temperatures in both solution (25 and 50 %). In 75 % and neat [C_4bim]Br (Figures SS2C and SS2D in Supporting Information), despite temperature increases, low fluctuations of DNA bases were still observed, demonstrating the rigidity of duplex DNA, leading to the assumption that 75 % and 100 % [C_4bim]Br solutions might be able to prevent the opening of DNA strands at high temperatures.

To prove the opening of DNA strands, the average of Watson-Crick hydrogen bonds between base pairs was calculated (Table 2). The average number of hydrogen bonds decreased when the temperature increased from 298.15 to 373.15 K. The average number of hydrogen bonds between DNA strands in 75 % [C_4bim]Br solution slightly reduced as compared to DNA in 50 and 25 % of [C_4bim]Br, showing that increasing concentrations of [C_4bim]Br helps to maintain the Watson-Crick hydrogen bonds and prevent the opening of base pairs. This fact can be correlated with the low RMSD value (refer back Figure 4), which indicated that the unfolding/denaturation of DNA in ILs are avoided at high temperatures. For DNA in aqueous solution, the average number of hydrogen bonds greatly decreased, indicating the separation of some of the base pairs.

As molecules of ILs have hydrogen bond donors/acceptors, they may be able to engage in inter-hydrogen bonding with the bases of the DNA helix, thus helping to maintain its double-helix structure. Increasing simulation temperatures from 298.15 to 373.15 K slightly increases the average number of hydrogen bonds for both cations and anions (Table SS3 in Supporting Information file). For DNA in hydrated IL system, increasing the percentage of [C_4bim]Br leads to an increase in the number of hydrogen bonds. The average number of hydrogen bonds is almost unchanged for the system containing 25 and 50 % and slightly increases for the system 75 % and neat [C_4bim]Br when the temperature increases from 298.15 K to 373.15 K.

Table 2 Average number of Watson-Crick hydrogen bonds of DNA strands at different percentages of [C_4bim]Br (% w/w) and various temperatures. Hydrogen bonds are considered when the distances between the donor and the acceptor less than 0.35 nm and the angle hydrogen-donor-acceptor is lower than 30°. Average hydrogen bonds of DNA strands in aqueous system were also calculated for the purpose of comparison. Data averaged over the last 2 ns of MD simulations.

System	[IL]:H_2O (% w/w)	Temperature (K)			
		298.15	323.15	343.15	373.15
H_2O	0:100	31.9 ± 1.9	27.6 ± 1.5	28.1 ± 1.6	24.7 ± 1.8
[C_4bim]Br	25:75	32.0 ± 1.8	29.0 ± 1.2	28.5 ± 1.4	27.3 ± 1.7
[C_4bim]Br	50:50	32.0 ± 0.9	31.0 ± 1.3	29.1 ± 1.3	28.4 ± 1.4
[C_4bim]Br	75:25	32.0 ± 1.1	30.6 ± 1.3	30.4 ± 1.5	30.0 ± 1.8
[C_4bim]Br	100:0	32.0 ± 1.3	31.5 ± 1.6	31.3 ± 1.4	31.2 ± 1.8

The number of Watson-Crick hydrogen bonds between the two strands in the initial crystal structure is 32.

This proved that temperature does not affect the formation of inter-hydrogen bonds between DNA bases and IL's ions. The hydrogen bonds were well preserved at higher temperatures, perhaps due to the thermal stability of ILs. The number of hydrogen bonds formed was found to be two or three times higher between DNA bases and cations than anions. DNA is well known as a poly-anion polymer, thus it is not surprising that the cations are well-distributed than anions on the surface of DNA, thus form more hydrogen bonding interaction.

3.2 Experimental Verifications

3.2.1 Fluorescence Study

Fluorescence experiments were performed to validate the findings of MD simulations. Generally, the emission intensity of certain molecules such as ligands will increase upon the addition of DNA. The increases in intensity demonstrate that molecules have an ability to bind with DNA. In this work, the emission intensity of $[C_4bim]Br$ increased when DNA was added, indicating that there was an interaction between ILs and duplex DNA (Figure 10). As reported, the dominant mode binding is electrostatic interaction between ILs' cations and DNA phosphate groups.[31,33,37] It is possible that ILs also can bind in an another mode with DNA, as is the case with other types of molecules.

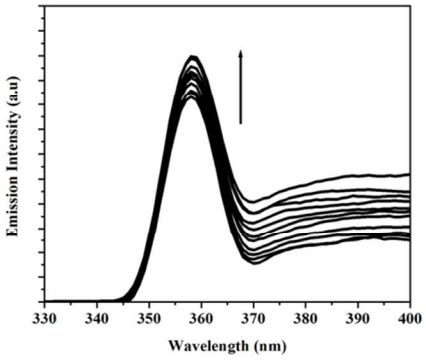

Fig. 10 Fluorescence spectra of $[C_4bim]Br$ in the absence (bottom curve) and presence of Ct-DNA in aqueous solution of deionized water contained 8 % ethanol. The arrow indicates that the emission intensity of $[C_4bim]Br$ increases with increasing DNA concentration. Excitation wavelength for $[C_4bim]Br$ was set at 320 nm.

Based on MD simulation results, IL cations were located at the backbone and in both major and minor grooves. With the addition of DNA, cations will bind to the interior, electronegative sites of the grooves. The bases of DNA in the major and minor grooves serve as a protector for nitrogen in the ring of $[C_4bim]^+$ from bulk water molecules, which enhances the emission intensity. Bathochromic shifts are not observed upon the addition of DNA into the $[C_4bim]Br$ solution. This indicates that intercalation is not the probable binding mode. Generally, bathochromic effects are the result of intercalation of molecules into DNA grooves. Small $[C_4bim]^+$ molecules can enter the grooves easily without altering the DNA structure. The interaction between DNA bases and cations was sufficiently strong to prevent hydrogen bonding interaction between water and nitrogen in $[C_4bim]^+$.

Fluorescence quenching of DNA-bound pyrene induced by $[C_4bim]Br$ was also performed (Figure 11). When $[C_4bim]Br$ was titrated into the solution of DNA-bound pyrene, electrostatic interactions occur between cations and DNA phosphate groups, which can also occur inside the grooves. As reported by Pullman et al.[59] the negative charge of DNA is greater in the A-T minor grooves rather than in the major grooves. It is well known that there are intercalations of pyrene with DNA bases at the grooves. The resulting electrostatic interaction leaves insufficient space for pyrene as $[C_4bim]Br$ is able to compete with pyrene to bind with DNA. Pyrene is gradually released from the grooves into bulk water when $[C_4bim]Br$ is added, therefore increasing the emission intensity of free pyrene was observed. The increase in the fluorescence emission of pyrene indicates that the interaction between ILs' cations and DNA was adequately strong to displace the intercalation of pyrene in duplex DNA.

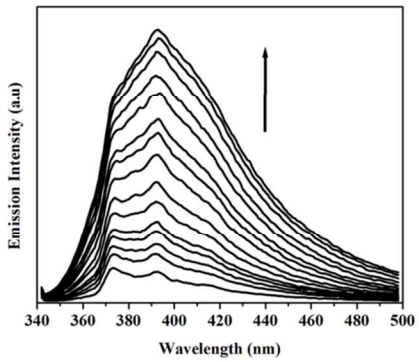

Fig. 11 Fluorescence emission spectra of free pyrene from DNA-bound pyrene solution quenched by $[C_4bim]Br$ at 25 °C. The arrow shows the increased emission intensity of free pyrene upon the addition of $[C_4bim]Br$.

3.2.2 Circular Dichroism Spectra

The spectra of the secondary structure of Ct-DNA in the presence of different percentages of $[C_4bim]Br$ were detected using circular dichroism. As shown in Figure 12, the characteristic positive band at around 278 nm corresponding to π-π base packing and a shortwave, negative band at 243 nm corresponding to helicity were present in all systems at 25 °C. Both positive and negative bands confirmed the presence of B-form duplex DNA.[60] The CD spectra of Ct-DNA in different percentages of $[C_4bim]Br$ shows a shape similar to that of pure DNA in deionized water at 25 °C, indicating that the duplex B-conformation DNA retains its shape in hydrated $[C_4bim]Br$ despite the high salt concentration.

Upon the addition of $[C_4bim]Br$, magnitudes of the positive band remained constant, but there was a slight decrease in the negative band, which may be due to the strong interactions of ILs' cations with Ct-DNA, which could lead to a transition from the extended double helix to the more compact form known as the Ψ structure.[61] The absence of any induced signal in the

spectra of Ct-DNA with the addition of [C_4bim]Br indicates that IL is not an intercalator. Intercalation usually induces the magnitude of positive and negative bands of DNA.[62] Based on the experimental data available, it was concluded that ILs, especially those based on alkylimidazolium cations do not intercalate with the bases of duplex DNA, but bind to DNA bases through groove binding and hydrophobic interactions. These bindings and major electrostatic interactions help to stabilize DNA and retain its duplex conformation in neat and hydrated ILs.

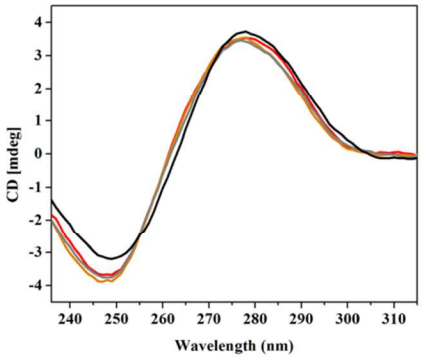

Fig. 12 CD spectra of Ct-DNA (300 µM) in deionized water and in different percentages of hydrated [C_4bim]Br at 25 °C. Colour scheme: black, control DNA in deionized water; red, 25 %; gray, 50%; orange, 75 % [C_4bim]Br.

4. Conclusion

The structural stability of DNA in ILs was discussed on the basis of results from MD simulations and experimental evidence. The effect of ILs, in particular, cations on the stability of DNA was studied in the presence of neat and hydrated ILs. The DNA conformation was found closer to its native structure in the presence of hydrated ILs at low water percentages and the stability of duplex DNA was mainly depends on the hydration shells at the surface of the DNA. Further study revealed that the entropy of water was found to play an important role in destabilizing the double helical DNA structure. However, this phenomenon was not observed in high percentage of ILs solution (75 % [C_4bim]Br). Low root mean square deviation (RMSD) of DNA was observed in this solution at high temperatures up to 373.15 K, indicated that ILs are also able to stabilize and maintain the native B-conformation DNA at high temperature. It was found that the dominant interaction for stabilizing the Ct-DNA was the electrostatic attraction between the head charge group of cations and the DNA phosphate groups. All the MD simulation results were in agreement with experimental evidences.

Acknowledgements

This work was in part financially supported by FCT PEst-C/QUI/UI0686/2011 and FCOMP-01-0124-FEDER-022716, Portugal and Research University Grant Scheme (RUGS), Universiti Putra Malaysia, Malaysia. The authors thank the access to the Minho University GRIUM cluster and for contract research grant C2008-UMINHO-CQ-03. K. Jumbri acknowledges the National Science Fellowship, MOSTI. M.B. Abdul Rahman acknowledges Genetic and Molecular Biology Iniative, MGI, Malaysia.

Notes and references

[a] Department of Chemistry, Faculty of Science, Universiti Putra Malaysia, 43400 UPM Serdang, Selangor, Malaysia
[b]Enzyme and Microbial Technology Research Centre (EMTech), University Putra Malaysia, 43400 UPM Serdang, Selangor, Malaysia.
[c] Chemistry Centre, Minho University, Campus Gualtar, 4710-057 Braga, Portugal. Fax: +351 253 60 4382; Tel: +351 253 60 4370; E-mail: micaelo@quimica.uminho.pt

Electronic Supplementary Information (ESI) available: File containing details of force fields parameterization and validation of [C_2bim]Br, [C_4bim]Br and [C_6bim]Br. Figure SS1 illustrates DNA structure in different simulation systems. Figure SS2 shows the root mean square fluctuations (RMSF) of DNA bases in neat and hydrated [C_4bim]Br. Table SS1 giving the number of [C_4bim]Br and water molecules around DNA surface. Table SS2 lists calculated interaction energies between different parts in the simulation systems. Table SS3 lists a number of inter-hydrogen bonding between [C_4bim]Br and DNA bases. See DOI: 10.1039/b000000x/

1. M. Lukin and C. de los Santos, *Chem. Rev.* 2006, **106**, 607.
2. Y.-K. Cheng and B. M. Pettitt, *Prog. Biophys. Mol. Bio.*1992, **58**, 225.
3. T. Lindahl and B. Nyberg, *Biochemistry* 1972, **11**, 3610.
4. D. Müller, B. Hofer, A. Koch and H. Köster, *BBA-Gene Struct. Expr.*1983, **740**, 1.
5. C. G. Albarino and V. Romanowski, *Mol. Cell. Probe.*1994, **8**, 423.
6. M. Matsumoto, K. Mochiduki and K. Kondo, *J. Biosc. Bioeng.*2004, **98**, 344.
7. G. Bonner and A. M. Klibanov, *Biotechnol. Bioeng.*2000, **68**, 339.
8. B. Hammouda and D. Worcester, *Biophys. J.* 2006, **91**, 2237.
9. R. Vijayaraghavan, A. Izgorodin, V. Ganesh, M. Surianarayanan and D. R. MacFarlene, *Angew. Chem. Int. Edit.*2010, **49**, 1631.
10. B. Röder, K. Frühwirth, C. Vogl, M. Wagner and P. Rossmanith, *J. Clin. Microbiol.*2010, **48**, 4260.
11. J. Bonnet, M. Colotte, D. Coudy, V. Couallier, J. Portier, B. Morin and S. Tuffet, *Nucleic Acids Res.* 2010, **38**, 1531.
12. J. G. Huddleston, A. E. Visser, W. M. Reichert, H. D. Willauer, G. A. Broker and R. D. Rogers, *Green Chem.* 2001, **3**, 156.
13. Y. He, Z. Li, P. Simone and T. P. Lodge, *J. Am. Chem. Soc.* 2006, **128**, 2745.
14. T. Welton, *Chem. Rev.* 1999, **99**, 2071.
15. T. D. Avery, N. F. Jenkins, M. C. Kimber, D. W. Lupton and D. K. Taylor, *Chem. Commun.*2002, 28.
16. J. G. Huddleston, H. D. Willauer, R. P. Swatloski, A. E. Visser and R. D. Rogers, *Chem. Commun.*1998, 1765.
17. M. Smietana and C. Mioskowski, *Org. Lett.*2001, **3**, 1037.
18. K. Fukumoto, M. Yoshizawa and H. Ohno, *J. Am. Chem. Soc.* 2005, **127**, 2398.
19. A. M. Leone, S. C. Weatherly, M. E. Williams, H. H. Thorp and R. W. Murray, *J. Am. Chem. Soc.* 2001, **123**, 218.

20. P. Wasserscheid and W. Keim, *Angew. Chem. Int. Edit.*2000, **39**, 3773.
21. J. L. Anderson, J. Ding, T. Welton and D. W. Armstrong, *J. Am. Chem. Soc*. 2002, **124**, 14247.
22. S. Chun, S. V. Dzyuba and R.A Bartsch, *Anal. Chem*. 2001, **73**, 3737.
23. L. A. Blanchard and J. F. Brennecke, *Ind. Eng. Chem. Res.* 2001, **40**, 287.
24. K.-S. Kim, D. Demberelnyamba and H. Lee, *Langmuir* 2004, **20**, 556.
25. Y. Zhou and M. Antonietti, *J. Am. Chem. Soc*. 2003, **125**, 14960.
26. A. Taubert, *Angew. Chem. Int. Edit.* 2004, **43**, 5380.
27. T. Brezesinski, C. Erpen, K.-I, Iimura and B. Smarsly, *Chem. Mater.*2005, **17**, 1683.
28. C. W. Scheeren, G. Machado, J. Dupont, P. F. P. Fichtner, S. Ribeiro Texeira,*Inorg. Chem*. 2003, **42**, 4738.
29. W. Qin and S. F. Y. Li, *Analyst* 2003, **128**, 37.
30. N. Nishimura, Y. Nomura, N. Nakamura and H. Ohno, *Biomaterials* 2005, **26**, 5558.
31. J.-H. Wang, D.-H.Cheng, X.-W.Chen, Z. Du and Z.-L. Fang, *Anal. Chem*. 2007, **79**, 620.
32. W. Sun, Y. Li, M. Yang, S. Liu and K. Jiao, *Electrochem. Commun.*2008, **10**, 298.
33. Y. Ding, L. Zhang, J. Xie and R. Guo, *J. Phys. Chem. B* 2010, **114**, 2033.
34. L. Cardoso and N. M. Micaelo, *ChemPhysChem*2011, **12**, 275.
35. A. Chandran, D. Ghoshdastidar and S. Senapati, *J. Am. Chem. Soc.* 2012, **134**, 20330.
36. H. Rozenberg, D. Rabinovich, F. Frolow, R. S. Hegde, Z. Shakked, *Proc. Natl. Acad. Sci. USA,* 1998, **95**, 15194.
37. H. Wang, J. Wang and S. Zhang, *Phys. Chem. Chem. Phys.* 2011, **13**, 3906.
38. N. M. Micaelo, A. M. Baptista, C. M. Soares, *J. Phys. Chem. B* 2006, **110**, 14444.
39. T. Darden, D. York and L. Pedersen, *J. Chem. Phys*. 1993, **98**, 10089.
40. U. Essmann, L. Perera, M. L. Berkowitz, T. Darden, H. Lee and L. G. Pedersen, *J. Chem. Phys*. 1995, **103**, 8577.
41. B. Hess, H. Bekker, H. J. C. Berendsen and J. G. E. M. Fraaije, *J. Comput. Chem.* 1997, **18**, 1463.
42. H. J. C. Berendsen, J. P. M. Postma, W. F. Van Gunsteren, A. Dinola, J. R. Haak, *J. Chem. Phys*. 1984, **81**, 3684.
43. W. L. DeLano, The PyMOL Molecular Graphics System. DeLano Scientific LLC, Palo Alto, CA, USA, 2008.
44. J. Wang, H. Wang, S. Zhang, H. Zhang and Y. Zhao, *J. Phys. Chem. B* 2007, **111**, 6181.
45. J. D. Knight and R. C. Adami, *Int. J. Pharm.* 2003, **264**, 15.
46. M. E. Reichmann, S. A. Rice, C. A. Thomas and P. Doty, *J. Am. Chem. Soc*. 1954, **76**, 3047.
47. K. Fujita, D. R. MacFarlene and M. Forsyth, *Chem. Commun.*2005, 4804.
48. R. Vijayaraghavan, B. C. Thompson, D. R. MacFarlene, R. Kumar, M. Surianarayanan, S. Aishwarya and P. K. Sehgal, *Chem. Commun.*2010, **46**, 294.
49. K. Fujita, D. R. MacFarlene, M. Forsyth, M. Yoshizawa-Fujita, K. Murata, N. Nakamura and H. Ohno, *Biomacromolecules* 2007, **8**, 2080.
50. G. S. Edwards, C. C. Davis, J. D. Saffer and M. L. Swicord, *Phys. Rev. Lett.*1984, **53**, 1284.
51. B. Schneider, K. Patel and H. M. Berman, *Biophys. J.* 1998, **75**, 2422.
52. B. Hammouda, *Int. J. Biol. Macromol.*2009, **45**, 532.
53. H. R. Drew and R. E. Dickerson, *J. Mol. Biol*. 1981, 151, 535.
54. S. Arai, T. Chatake, T. Ohhara, K. Kurihara, I. Tanaka, N. Suzuki, Z. Fujimoto, H. Mizuno and N. Niimura, *Nucleic Acids Res*. 2005, **33**, 3017.
55. B. Schneider, K. Patel and H. M. Berman, *Biophys. J.* 1998, **75**, 2422.
56. N. Korolev, A. P. Lyubartsev, A. Laaksonen and L. Nordenskiöld, *Nucleic Acids Res.* 2003, **31**, 5971.
57. M. Egli, V. Tereshko, M. Teplova, G. Minasov, A. Joachimiak, R. Sanishvili, C. M. Weeks, R. Miller, M. A. Maier and H. An, *Biopolymers* 1998, **48**, 234.
58. P. Auffinger and E. Westhof, *Biophys. Chem.* 2002, **95**, 203.
59. A. Pullman and B. Pullman, *Q. Rev. Biophys.*1981, **14**, 289.
60. M. Cao, M. Deng, X.-L. Wang and Y. Wang, *J. Phys. Chem. B* 2008, **112**, 13648.
61. C. F. Jordan, L. S. Lerman and J. H. Venable, *Nature-New Biol.* 1972, **236**, 67.
62. S. Parodi, F. Kendall and C. Nicolini, *Nucleic Acids Res.* 1975, **2**, 477.

Insight into Structure and Stability of DNA in Ionic Liquids from Molecular Dynamics Simulation and Experimental Studies

K. Jumbri,[a,b] M. B. Abdul Rahman,[a,b] E. Abdulmalek,[a,b] H. Ahmad[a,b] and N. M. Micaelo[c,*]

Keywords: Ionic liquids, DNA, Stability, Hydration shells, molecular dynamics

Table of Content

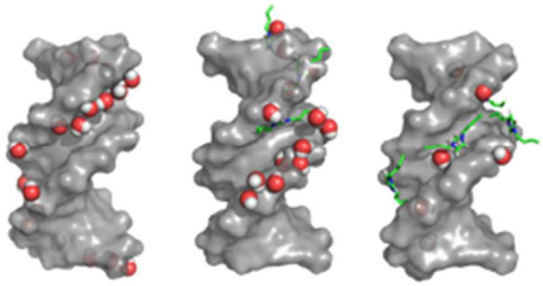

Hydration shells on DNA surface are the main criterion in determine the DNA stability with the weaker hydration shells increase the binding ability of ionic liquids to DNA